J|A|C|S
ARTICLES

Published on Web 04/16/2008

Functionalized Methanofullerenes Used as n-Type Materials in Bulk-Heterojunction Polymer Solar Cells and in Field-Effect Transistors

Changduk Yang,[†] Jin Young Kim,[‡] Shinuk Cho,[‡] Jae Kwan Lee,[‡] Alan J. Heeger,[‡] and Fred Wudl*[,†,‡]

Mitsubishi Chemical Center for Advanced Materials and Department of Chemistry and Biochemistry and Center for Polymers and Organic Solids, University of California, Santa Barbara, California 93106

Received November 27, 2007; E-mail: wudl@chem.ucsb.edu

Abstract: The synthesis of two well-solubilized [60]methanofullerene derivatives (*p*-**EHO-PCBM** and *p*-**EHO-PCBA**) is presented for usage in organic solar cells and in field-effect transistors. The para position of the PCBM's phenyl ring was substituted with a branched alkoxy side chain, which contributes to higher solubility, facilitating synthesis, purification, and processing. We find a small change of the open-circuit voltage (V_{oc}) as a slight improvement in performance upon application in P3HT/[60]methanofullerene bulk-heterojunction-photovoltaic cells, when compared to PCBM, because of the electron donation of the alkoxy group. In the case of the devices with a TiO_x layer, the best power conversion efficiencies (PCE, η_e) is observed in a layered structure of P3HT/*p*-**EHO-PCBA**/TiO_x ($\eta_e = 2.6\%$), which slightly exceeds that of P3HT/PCBM/TiO_x ($\eta_e = 2.3\%$) under conditions reported here. This can be attributed, in part, to the carboxylic acid group in *p*-**EHO-PCBA** that leads to an effective interface interaction between the active layer and TiO_x phase. In addition, n-channel organic field-effect transistor (OFET) devices were fabricated with thin films of *p*-**EHO-PCBM** and *p*-**EHO-PCBA**, respectively cast from solution on SiO_2/Si substrates. The values of field-effect mobility (μ) for *p*-**EHO-PCBM** and *p*-**EHO-PCBA** are 1×10^{-2} and 1.6×10^{-3} $cm^2/V \cdot s$, respectively. The results in this paper demonstrate the effects of a carboxylic acid group and an electron-donating substituent in [60]methanofullerenes as n-type materials with respect to organic solar cells and OFET applications.

Introduction

The possibility to use new organic semiconductor materials in place of silicon wafers in the fabrication of photovoltaic cells offers the prospects of lower manufacturing costs (printing and coating technologies using solution-processable materials), lightweight solar modules, and flexible large-area applications.[1] Thus, one of the most promising opportunities in [60]fullerene research[2] involves the potential application, when mixed with π-conjugated polymers, in mimicking photosynthesis and in related solar-energy conversion.[3,4] The most widely used configuration of polymer solar cells is the so-called bulk-heterojunction device, in which the active layer consists of a blend of electron-donating materials, for example, p-type conjugated polymers, and an electron-accepting material (n-type) such as (6,6)-phenyl C_{61}-butyric acid methyl ester (PCBM).[5,6] Organic solar cells with power conversion efficiencies (PCE) approaching 5% under AM1.5G illumination have recently been reported by using a regioregular poly(3-hexylthiophene) (rr-P3HT)/PCBM blend[7–9] and by introducing morphology-improving procedures on the composite film.[10–13] Several factors are important in further improving the efficiency of an organic solar cell. Among these, the development of an electron-donating polymer with low band gap to efficiently absorb light in the visible area of the solar spectrum and structural manipulation

[†] Mitsubishi Chemical Center for Advanced Materials and Department of Chemistry and Biochemistry.
[‡] Center for Polymers and Organic Solids.

(1) Gunes, S.; Neugebauer, H.; Sariciftci, N. S. *Chem. Rev.* **2007**, *107*, 1324.
(2) Sariciftci, N. S.; Smilowitz, L.; Heeger, A. J.; Wudl, F. *Science* **1992**, *258*, 1474.
(3) Brabec, C. J.; Dyakonov, V.; Parisi, J.; Sariciftci, N. S. *Organic Photovoltaics. Concepts and Realizations*; Springer: Berlin, 2003.
(4) Yu, L.; Gao, L.; Hummelen, J. C.; Wudl, F.; Heeger, A. J. *Science* **1995**, *270*, 1789.
(5) Hummelen, J. C.; Knight, B. W.; LePeq, F.; Wudl, F.; Yao, J.; Wilkins, C. L. *J. Org. Chem.* **1995**, *60*, 532.
(6) Janssen, R. A. J.; Hummelen, J. C.; Lee, K.; Pakbaz, K.; Sariciftci, N. S.; Heeger, A. J.; Wudl, F. *J. Chem. Phys.* **1995**, *103*, 788.
(7) Li, G.; Shrotriya, V.; Huang, J.; Yao, Y.; Moriarty, T.; Emery, K.; Yang, Y. *Nat. Mater.* **2005**, *4*, 864.
(8) Ma, W.; Yang, C.; Gong, X.; Lee, K.; Heeger, A. J. *Adv. Funct. Mater.* **2005**, *15*, 1617.
(9) Reyes-Reyes, M.; Kim, K.; Carroll, D. L. *Appl. Phys. Lett.* **2005**, *87*, 083506.
(10) Wienk, M. M.; Kroonm, J. M.; Verhees, W. J. H.; Knol, J.; Hummelen, J. C.; van Hal, P. A.; Janssen, R. A. J. *Angew. Chem., Int. Ed.* **2003**, *42*, 3371.
(11) Chirvase, D.; Chiguvare, Z.; Knipper, M.; Parisi, J.; Dyakonov, V.; Hummelen, J. C. *J. Appl. Phys.* **2003**, *93*, 3376.
(12) Camaioni, N.; Ridolfi, G.; Casalbore-Miceli, G.; Possamai, A.; Maggini, M. *Adv. Mater.* **2002**, *14*, 1735.
(13) Padinger, F.; Rittberger, R.; Sariciftci, N. S. *Adv. Funct. Mater.* **2003**, *12*, 85.

10.1021/ja710621j CCC: $40.75

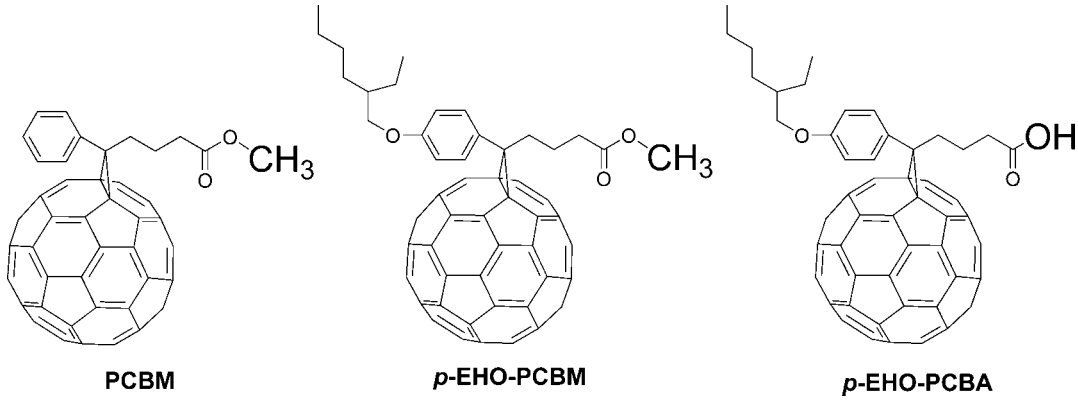

Figure 1. Structure of PCBM, *p*-**EHO-PCBM**, and *p*-**EHO-PCBA**.

of the acceptor component to optimize the solar cell performance are important. Therefore, there is still plenty of room to tune the efficiencies of bulk-heterojunction photovoltaic cells.

Not only have we previously developed the architecture for high-efficiency polymer photovoltaic cells by using TiO_x as an optical spacer,[14] but Fréchet et al.[15] have also reported that carboxylic acid functionalized polythiophene/TiO_2 cell enables improvement of the performance through the interface interaction between the polymer and TiO_2. More recently, it was noted that placing electron-donating substituents on the phenyl ring of PCBM can raise the lowest unoccupied molecular orbital (LUMO) of PCBM, which allows further optimization of the open-circuit voltage (V_{oc}) of polymer/[60]fullerene organic solar cells.[16]

In addressing these issues, we directed our attention toward the synthesis of [60]methanofullerene analogues with the following points in mind: (i) the introduction of a branched alkoxy side chain as an electron-donating solubilizer on the phenylene of PCBM (*p*-**EHO-PCBM**; this change was expected not only to contribute to easier solution processability but also to potentially increase the open-circuit voltage (V_{oc})) and (ii) the availability in *p*-**EHO-PCBA** of a carboxylic acid group as an important functionality for potential interaction with oxides. This is important because it enables us to study the solar cell performance with a comparison between a carboxylate ester and a carboxylic acid in conventional and TiO_x layer devices, which, to the best of our knowledge, has not been investigated so far (Figure 1).

Herein, we describe the synthesis and application in bulk-heterojunction solar cells as well as field-effect transistors (FETs)[17,18] of the above-mentioned novel solution-processable [60]methanofullerene analogues (*p*-**EHO-PCBM** and *p*-**EHO-PCBA**) in combination with P3HT.

Results and Discussion

The synthetic approach to *p*-ethylhexyloxy-substituted [60]methanofullerene derivatives (*p*-**EHO-PCBM** and *p*-**EHO-PCBA**) is depicted in Scheme 1. The 4-(2-ethyl-hexyloxy) benzoylbutyric acid (**1**) was prepared by $AlCl_3$-promoted Friedel−Crafts acylation of 2-ethylhexyloxy benzene[19] with glutaric anhydride (31%). The benzoylbutyric acid **1** was then converted to the methyl 4-(2-ethyl-hexyloxy) benzoylbutyrate (**2**) in methanol under Fischer esterification conditions (98%).

The synthesis of *p*-**EHO-PCBM** was carried out by the Wudl−Hummelen approach.[5] Condensation of **2** with *p*-tosylhydrazide in methanol afforded the corresponding *p*-tosylhydrazone compound (**3**), which after sequential treatment with sodium methoxide in pyridine and [60]fullerene in refluxing *o*-dichlorobenzene (*o*-DCB) gave fullerene derivative **4** in 34% isolated yield. Although both [6,6]-closed and [5,6]-open isomers could be expected from the cycloaddition reaction, the high temperature at which the reaction proceeds allowed the isolation of the thermodynamically more stable [6,6]-closed isomer, exclusively, as determined by ^{13}C NMR. The ester was hydrolyzed with hydrochloric acid/acetic acid to the corresponding *p*-**EHO-PCBA** (96%). Both [60]methanofullerene analogues (*p*-**EHO-PCBM** and *p*-**EHO-PCBA**) were readily soluble in common organic solvents (THF, dichloromethane, toluene, *o*-DCB, etc.).

Electrochemical Properties. The electrochemical properties of *p*-**EHO-PCBM** and *p*-**EHO-PCBA** were studied by cyclic voltammetry (CV) at room temperature in *o*-DCB solution. The experiments were carried out by using tetra-*n*-butylammonium perchlorate (Bu_4NClO_4, 0.1 M) as the supporting electrolyte, a platinum working electrode, a platinum wire as the counter electrode, and Fc/Fc^+ as the internal reference.

Not only does the cyclic voltammogram of *p*-**EHO-PCBM** and *p*-**EHO-PCBA** show three reduction waves, but also all reductions exhibit clear quasireversibility (see Supporting Information). The CV data are summarized in Table 1, where E^1_{red}, E^2_{red}, and E^3_{red} reduction potentials (defined as $E_{red} = 0.5(E_{pa} + E_{pc})$) are listed together with [60]fullerene and PCBM data obtained in this study for comparison. The reduction potentials of [60]methanofullerene analogues are shifted to more negative values with respect to C_{60} because of the decrease of the number of π-electrons and the release of strain energy.[20,21]

In the case of *p*-**EHO-PCBM** and *p*-**EHO-PCBA**, the reduction values are slightly more negative than those of PCBM. This could be attributed to the inductive effect of the alkoxy group on the redox behavior. It was reported that, within similar

(14) Kim, J. Y.; Kim, S. H.; Lee, H.-H.; Lee, K.; Ma, W.; Gong, X.; Heeger, A. J. *Adv. Mater.* **2006**, *18*, 572.
(15) Liu, J.; Kadnikova, E. N.; Liu, Y.; McGehee, M. D.; Fréchet, M. J. *J. Am. Chem. Soc.* **2004**, *126*, 9486.
(16) Kooistra, F. B.; Knol, J.; Kastenberg, F.; Popescu, L. M.; Verhees, W. J. H.; Kroon, J. M.; Hummelen, J. C. *Org. Lett.* **2007**, *9*, 551.
(17) Nakamura, J.; Murata, K.; Takahashi, K. *Appl. Phys. Lett.* **2005**, *87*, 132105.
(18) Shibao, M.; Morita, T.; Takahashi, K.; Kaneto, K. *Jpn. J. Appl. Phys.* **2007**, *46*, L123.
(19) Kim, S. W.; Shim, S. C.; Jung, B. J.; Shim, H. K. *Polymer* **2002**, *43*, 4297.
(20) Haddon, R. C. *Science* **1993**, *261*, 545.
(21) Lamparth, I.; Hirsch, A. *J. Chem. Soc., Chem. Commun.* **1994**, 1727.

Scheme 1. Synthesis of [60]Methanofullerene Derivatives (***p*-EHO-PCBM** and ***p*-EHO-PCBA**)

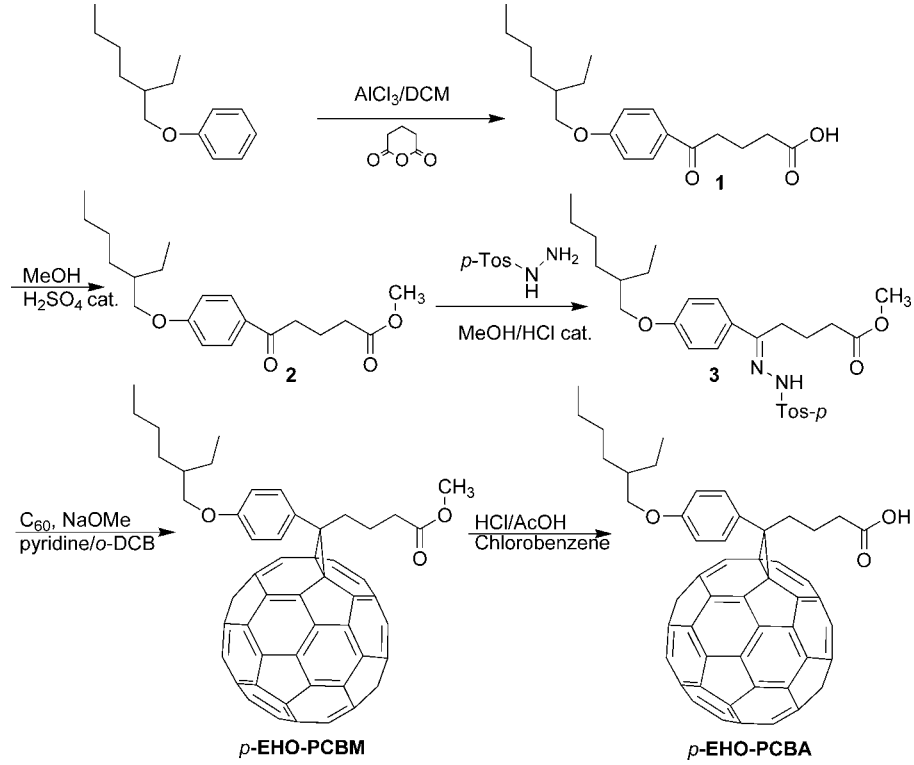

Table 1. Electrochemical Data[a]

compound	E^1_{red}	E^2_{red}	E^3_{red}
***p*-EHO-PCBM**	−1.171	−1.544	−2.048
***p*-EHO-PCBA**	−1.181	−1.565	−2.087
PCBM	−1.163	−1.538	−2.040
C_{60}	−1.077	−1.456	−1.914

[a] Experimental conditions: values for $0.5(E_{pa} + E_{pc})$ in V vs Fc/Fc+; 10^{-4} to 10^{-3} mol/L *o*-DCB solution; Bu_4NClO_4 (0.1 M) as supporting electrolyte; Pt wire as counter electrode; 50 mV/s scan rate.

structure, the inductive effect by attached organic groups is the most important factor to determine the redox properties of organofullerene derivatives.[22] Furthermore, it has recently been proven that alkoxy groups on the phenyl ring of PCBM can lead to a decrease of the reduction potential.[16] A slightly decreased reduction potential of ***p*-EHO-PCBA** versus ***p*-EHO-PCBM** was also observed. As a result, it is expected that the LUMO levels of ***p*-EHO-PCBM** and ***p*-EHO-PCBA** are somewhat raised in comparison with the LUMO level of PCBM.

Film Morphology Study. The physical morphology of the thin films of the three blends of P3HT/PCBM, P3HT/***p*-EHO-PCBM**, and P3HT/***p*-EHO-PCBA**, observed by atomic force microscopy (AFM), are shown in Figure 2. All three spin cast films have smooth surfaces and remarkably similar features. The formation of voids, typically attributed to incompatibility between donor and acceptor components, is not observed. The rms roughness is 10.4 nm for P3HT/PCBM, 17.4 nm for P3HT/***p*-EHO-PCBM**, and 13.0 nm for P3HT/***p*-EHO-PCBA**. One possible conclusion is that the bulky solubilizing groups in ***p*-EHO-PCBM** and ***p*-EHO-PCBA** induce formation of a slightly larger feature size, when compared to PCBM, however without significant change in morphology.

Polymer Solar Cells. The polymer solar cells had a layered structure of glass/PEDOT:PSS/P3HT/[60]methanofullerene derivatives (PCBM, ***p*-EHO-**PCBM, and ***p*-EHO-PCBA**) blend/Al. The active layer was P3HT/[60]methanofullerenes respectively at 1:1 weight ratio. The blends were spin-coated from a solution containing the P3HT/[60]methanofullerenes in chloroform onto an ITO/glass substrate covered by a PEDOT:PSS (Baytron P) layer with a thickness of ∼100 nm that had previously been coated from aqueous solution.[23] In the case of the device with a TiO_x layer, the TiO_x precursor solution was applied in air on top of the P3HT/[60]methanofullerenes composition. Subsequently, a thin layer of aluminum was thermally deposited under vacuum. All data were obtained under white light AM1.5G illumination from a calibrated solar simulator with irradiation intensity of 100 mW/cm^2.

The device performance of a solar cell is determined by the open-circuit voltage (V_{oc}), short-circuit current density (J_{sc}), and fill factor (FF). The PCE (η_e) of a solar cell is given as $\eta_e = 100(J_{sc}V_{oc}FF)/P_{inc}$, where P_{inc} is the intensity of incident light. Higher values of those three parameters yield larger light-to-electricity PCE. The postproduction annealing at high temperature (∼150 °C) was performed because it has been proven to be a very efficient method for improving the electrical characteristics of P3HT/PCBM-based solar cells.[8,9,13]

Representative characteristics of the solar cells are listed in Table 2. The current−voltage curves of the solar cells based on the three blends P3HT/PCBM, P3HT/***p*-EHO-PCBM**, and P3HT/***p*-EHO-PCBA** are shown in Figure 3. The cell based on P3HT/PCBM serves as a standard reference for the comparison of the efficiencies with [60]methanofullerene analogues and has a short-circuit current density (J_{sc}) of 6.98 mA/cm^2, an open-circuit voltage (V_{oc}) of 0.60 V, and a fill factor (FF) of

(22) Suzuki, T.; Maruyama, Y.; Akasaka, T.; Ando, W.; Kobayashi, K.; Nagase, S. *J. Am. Chem. Soc.* **1994**, *116*, 1359.

(23) Al-Ibrahim, M.; Ambacher, O.; Sensfuss, S.; Gobsch, G. *Appl. Phys. Lett.* **2005**, *86*, 201120.

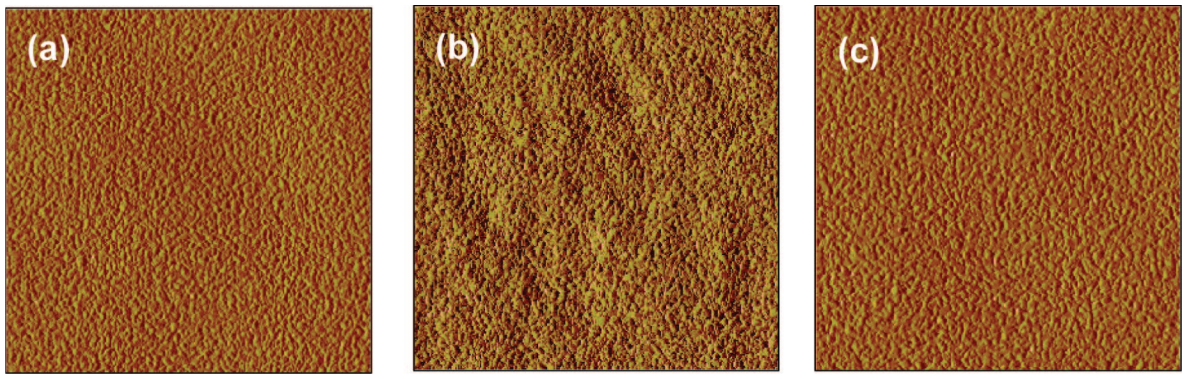

Figure 2. AFM topography images (5 μm × 5 μm) of films cast from chloroform solutions with (a) P3HT/PCBM, (b) P3HT/*p*-**EHO-PCBM**, and (c) P3HT/*p*-**EHO-PCBA**.

Table 2. Characteristics of Bulk-Heterojunction Polymer Solar Cells[a]

ratio (1:1)	J_{sc} (mA/cm^2)	V_{oc} (V)	FF	η_e (%)
P3HT/PCBM	6.98	0.60	0.43	1.81
P3HT/*p*-**EHO-PCBM**	4.43	0.65	0.35	1.01
P3HT/*p*-**EHO-PCBA**	5.83	0.64	0.46	1.73

[a] Short-circuit current density (J_{sc}), open-circuit voltage (V_{oc}), fill factor (FF), PCE (η_e) at P3HT as the electron donor/various acceptors (PCBM, *p*-**EHO-PCBM**, and *p*-**EHO-PCBA**) at weight ratio (1:1 w/w). The device performance was consistent and reproducible (see Experimental Section).

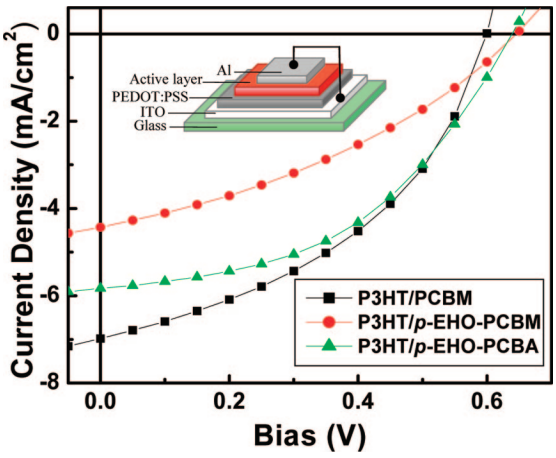

Figure 3. *J*−*V* characteristics of polymer solar cells under AM1.5G illumination from a calibrated solar simulator with an intensity of 100 mW/cm^2. Inset is a schematic of device architecture.

43%. Under the same white light illumination, the P3HT/*p*-**EHO-PCBM**-based cell exhibits a J_{sc} of 4.43 mA/cm^2, an open-circuit voltage (V_{oc}) of 0.65 V, and a fill factor (FF) of 35%. Its PCE (η_e) decreases to 0.80% in comparison with that of P3HT/PCBM, used as a reference. In the case of the solar cell made from P3HT/*p*-**EHO-PCBA**, the PCE (η_e) increases to 0.73%, a substantial improvement when compared to that of P3HT/*p*-**EHO-PCBM** but still slightly lower than that of P3HT/PCBM.

As expected, the V_{oc} values of both P3HT/*p*-**EHO-PCBM** and P3HT/*p*-**EHO-PCBA** are slightly improved in comparison with that of P3HT/PCBM because of the lower first potential reductions. This notion is supported by the linear correlation of the first reduction potential of [60]fullerene acceptors and

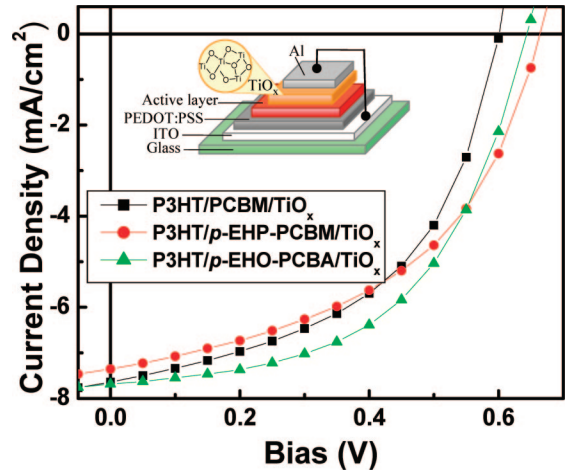

Figure 4. *J*−*V* characteristics of polymer solar cells with the TiO_x optical spacer under AM1.5G illumination from a calibrated solar simulator with an intensity of 100 mW/cm^2. Inset is a schematic of device architecture.

the observed V_{oc}.[24] In the case of both P3HT/*p*-**EHO-PCBM** and P3HT/*p*-**EHO-PCBA**, the significantly lower J_{sc} values lead to an overall decrease in PCE (η_e). This may be due to one of two factors: the blend layers are not uniform and changed into an undesirable nanomorphology because of the branched substituent, or the genetic character of alkoxy group causes a negative effect on the device. This assumption is substantiated by an AFM morphology study, in which the roughness of P3HT/PCBM appears better and smoother than those of P3HT/*p*-**EHO-PCBM** and P3HT/*p*-**EHO-PCBA**. Although the efficiencies of both P3HT/*p*-**EHO-PCBM** and P3HT/*p*-**EHO-PCBA** still can and need to be further improved with respect to high-end applications, the preliminary results can be comparable with that of the optimized high-performance polymer solar cell based on P3HT/PCBM.

We have recently demonstrated that introducing a TiO_x optical spacer to polymer photovoltaic cells results in PCEs that are increased by approximately 50%, compared to those of similar devices fabricated without the optical spacer.[14] To access optical interference effect on P3HT/*p*-**EHO-PCBM** and P3HT/*p*-**EHO-PCBA**, the devices with TiO_x as a spacer between the active layer and the Al electrode were fabricated (Figure 4), as described in the Experimental Section.

(24) Brabec, C. J.; Cravino, A.; Meissner, D.; Sariciftci, N. S.; Fromherz, T.; Minse, M.; Sanchez, L.; Hummelen, J. C. *Adv. Funct. Mater.* **2001**, *11*, 374.

Table 3. Characteristics of Bulk-Heterojunction Polymer Solar Cells with the TiO_x Optical Spacer[a]

ratio (1:1)	J_{sc} (mA/cm^2)	V_{oc} (V)	FF	η_e (%)
P3HT/PCBM/TiO_x	7.64	0.60	0.50	2.29
P3HT/*p*-**EHO-PCBM**/TiO_x	7.36	0.66	0.48	2.34
P3HT/*p*-**EHO-PCBA**/TiO_x	7.69	0.64	0.53	2.64

[a] Short-circuit current density (J_{sc}), open-circuit voltage (V_{oc}), fill factor (FF), PCE (η_e) at P3HT as the electron donor/various acceptors (PCBM, *p*-**EHO-PCBM**, and *p*-**EHO-PCBA**) at weight ratio (1:1 w/w). The device performance was consistent and reproducible (see Experimental Section).

The $J-V$ curves for devices with TiO_x layer obtained under white light illumination (AM1.5 G, 100 mW/cm) are shown in Figure 4, indicating a considerably improved performance. The corresponding PCEs (η_e) are 2.29, 2.34, and 2.64% for P3HT/PCBM, P3HT/*p*-**EHO-PCBM**, and P3HT/*p*-**EHO-PCBA**, respectively (Table 3). The TiO_x optical spacer leads to the overall increase in PCE (η_e) by creating more photogenerated charge carriers in the bulk-heterojunction layer, thereby increasing J_{sc}. Surprisingly, the TiO_x layer is more effective in enhancing the performance of the new [60]methanofullerene derivatives (*p*-**EHO-PCBM** and *p*-**EHO-PCBA**) in comparison to P3HT/PCBM.

The best performance is observed in the P3HT/*p*-**EHO-PCBA**/TiO_x heterojunction solar cell. This positive effect in photocurrent may be attributed to a combination of the following factors. The possibility of the chelation of carboxylic acids (−COOH) in *p*-**EHO-PCBA** to the TiO_x phase can contribute to this enhancement by promoting forward interfacial electron transfer, much in the same manner as in the Grätzel-type solar cells.[25,26] In addition, we cannot rule out that the branched alkoxy chain on the phenyl ring can produce an improved interface morphology between the active layer and TiO_x phases, which probably leads to the higher charge carrier mobility within the devices with TiO_x. We are currently studying the trend in device efficiency for [60]fullerene derivatives with various substitution patterns, in which energy effects and interaction effects can be separated, to help us better understand our observation.

n-Type Organic Field-Effect Transistors. To explore the electron transport properties of *p*-**EHO-PCBM** and *p*-**EHO-PCBA**, field-effect mobilities were investigated through the fabrication of n-type organic field-effect transistors (OFETs). All n-type OFETs were prepared on a heavily doped n^{++} Si wafer with a 200 nm thick thermally grown SiO_2 layer with top contact geometry as shown in Figure 5a. Ca was chosen as a metal for the source and drain electrodes to enable easy injection of electrons, because there is no energy barrier between the Ca electrode (the workfunction of Ca is 2.87 eV) and the active layer. A detailed fabrication process is described in the Experimental Section.

Figure 5b shows the transport characteristics of the n-type OFETs fabricated with *p*-**EHO-PCBM** and *p*-**EHO-PCBA**, compared to the n-type PCBM OFET. All $I_{ds}-V_{gs}$ curves are typical of good n-type OFETs, owing to the nature of [60]fullerene. The linear plot of $I^{1/2}$ versus V_{gs} (Figure 5c), deduced from the measurements of the I_{ds} versus V_{gs}, gave electron mobilities of $\mu_1 = 1.59 \times 10^{-3}$ cm^2/V·s, $\mu_2 = 1.04 \times 10^{-2}$ cm^2/V·s, and $\mu_3 = 2.85 \times 10^{-2}$ cm^2/V·s for the *p*-**EHO-PCBA**, *p*-**EHO-PCBM**, and PCBM, respectively. Such deterioration of the electron mobility in both *p*-**EHO-PCBM** and *p*-**EHO-PCBA** OFETs can be largely attributed to the bulkiness of the substituent that can suppress desirable ordering such as $\pi-\pi$ intermolecular overlaps between C_{60} moieties in the solid state. Among them, the lowest mobility value is observed in the *p*-**EHO-PCBA** OFET. This result currently lacks a theoretical explanation but can be due to the nature of the carboxylic acid group as an electron-trapping site. Further studies are required to assess more precisely the correlation between the size of substituents and/or the various functional groups and the mobility of an OFET. However, these mobilities are comparable to the typical values of the fullerene-based OFETs fabricated by vapor deposition under ultrahigh vacuum ($\mu = 8.0 \times 10^{-2}$ and 2.0×10^{-3} cm^2/V·s for C_{60} and C_{70}, respectively).[27,28] In the case reported here, the soluble [60]methanofullerene-based devices were fabricated by spin coating, which is easier and more cost-effective compared with vacuum deposition.

Conclusion

We have successfully synthesized a series of [60]methanofullerene analogues (*p*-**EHO-PCBM** and *p*-**EHO-PCBA**). The electrochemical studies show that both *p*-**EHO-PCBM** and *p*-**EHO-PCBA** undergo quasireversible processes. The introduction of a branched alkoxy substituent at the phenyl ring of [60]methanofullerenes not only renders these materials soluble and easily processable but also allows to access the influence of the carboxylic acid group in comparison with the methyl ester group in photovoltaic cells. Moreover, the alkoxy electron-donating ability leads to a slightly decreased reduction potential when compared to PCBM, resulting in somewhat improved V_{oc} values in the solar cell devices. By utilizing a TiO_x layer, the devices of P3HT/various acceptors (PCBM, *p*-**EHO-PCBM**, and *p*-**EHO-PCBA**) were also fabricated, resulting in significant enhancement of device performance. The corresponding PCEs (η_e) are 2.29% for PCBM, 2.34% for *p*-**EHO-PCBM**, and 2.64% for *p*-**EHO-PCBA**. The best solar cell obtained has a layered configuration of P3HT/*p*-**EHO-PCBA**/TiO_x, which can be attributed to the interface interaction between the active layer and the TiO_x phase. In addition, we cannot exclude that the branched solubilizing groups could tune the morphology of the active layers/TiO_x phase that can be responsible for the improvement of PCE (η_e).

In conclusion, through the structural manipulation of active layer materials, the interface interaction between active layer and TiO_x can be influenced, which can potentially enhance the solar cell performance. To further improve the device performance for such a bulk-heterojunction system, it is important to synthesize an acceptor that has high carrier mobility and good compatibility with the donor-type conjugated polymer simultaneously. The study of MEH-PPV/*p*-**EHO-PCBM** and *p*-**EHO-PCBA** as the acceptor is underway to further clarify the positive effect and the trend in both conventional and TiO_x-coated devices. As a separate work, n-type OFETs with *p*-**EHO-PCBM** and *p*-**EHO-PCBA** manufactured from solution have also been characterized. In a top-contact geometry, electron mobilities in the saturation regime were found to be $\mu = 1.04 \times 10^{-2}$ cm^2/V·s for *p*-**EHO-PCBM** and $\mu = 1.59 \times 10^{-3}$ cm^2/V·s for

(25) Grätzel, M. *Inorg. Chem.* **2005**, *44*, 6841.
(26) Moser, J.; Punchihewa, S.; Infelta, P. P.; Grätzel, M. *Langmuir* **1991**, *7*, 3012.
(27) Haddon, R. C. *J. Am. Chem. Soc.* **1996**, *118*, 3041.
(28) Haddon, R. C.; Perel, A. S.; Morris, R. C.; Palstra, T. T. M.; Hebard, A. F.; Fleming, R. M. *Appl. Phys. Lett.* **1995**, *67*, 121.

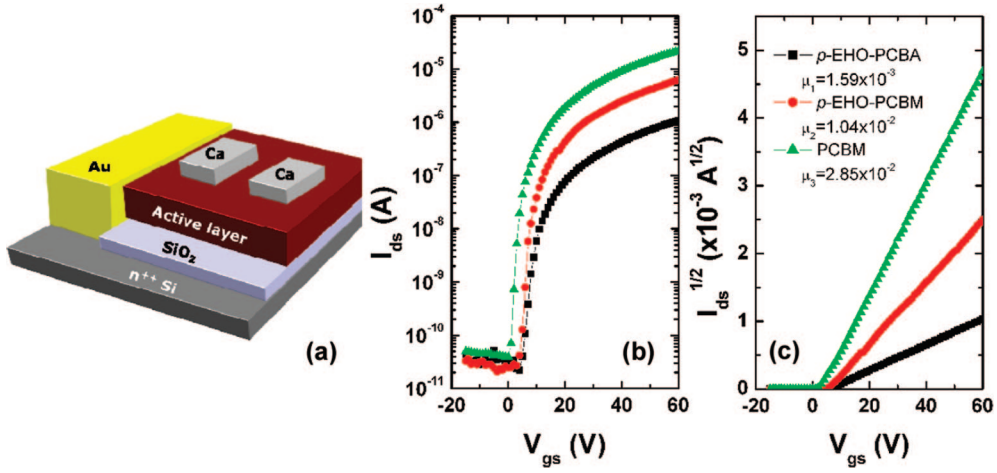

Figure 5. (a) Diagram of n-type OFET structure ($L = 50\ \mu$m, $W = 1.5$ mm). (b) Transfer characteristics of n-type OFETs. (c) $I^{1/2}$ versus V_{gs} plot. ▲, PCBM, ●, *p*-**EHO-PCBM**, ■, *p*-**EHO-PCBA**.

p-**EHO-PCBA**. Even though the OFET parameters are related to many factors, the present results indicate that the size and functionality of substituents could eventually lead to high-mobility fullerene derivatives.

Experimental Section

General. All solvents were purified and freshly distilled prior to use according to literature procedures. The synthesis of 2-ethylhexyloxy benzene was adapted from literature procedures.[19] Commercially available materials were used as received unless noted. ^{1}H and ^{13}C NMR spectra were recorded on a Varian Mercury Vx 200 MHz or Varian Unity Inova 500 MHz spectrometer and referenced to the solvent peak. Mass spectrometry and elemental analysis were performed by UC Santa Barbara Mass Spectrometry Laboratory and Elemental Analysis Center. The electrochemical measurements were carried out in *o*-DCB solution containing 0.1 M Bu_4NClO_4 as the supporting electrolyte, with Ag/AgCl as reference electrode and a platinum wire as a counter electrode and an internal ferrocene/ferrocenium standard. Anhydrous *o*-DCB was obtained from Aldrich and used as received. The AFM instrumentation consisted of a Nanoscope III BioScope system (Digital Instruments, Veeco Metrology Group, Santa Barbara, CA) and standard silicon tips (type OTESPA-70; L, 160 μm; normal spring constant, 50 N/m; resonance frequency, 246−282 kHz).

Solar Cell Device Fabrication and Calibration Procedure. Polymer solar cells were fabricated by using P3HT as the electron donor and [60]methanofullerene derivatives as the acceptor. The ITO-coated glass substrates were cleaned subsequently in an ultrasonic bath with detergent, distilled water, acetone, and isopropyl alcohol and then dried in an oven at ∼100 °C overnight. Highly conducting PEDOT:PSS was spin-cast (5000 rpm) with a thickness of ∼40 nm from aqueous solution after treatment of the ITO substrates with UV ozone for 40 min. The substrates were dried at 140 °C for 10 min in air and transferred to a nitrogen-filled glovebox for spin-casting the P3HT/[60]methanofullerene layer. The chloroform solution, comprising P3HT (1.0 wt%) and [60]methanofullerene derivatives (1.0 wt %), was spin-cast at 1200 rpm on top of the PEDOT:PSS layer. The thickness of the active layer was ∼100 nm. Then, the TiO_x (∼30 nm) was spin-cast (4000 rpm) on top of the P3HT/[60]methanofullerene composite from the 1 wt% precursor solution and heated at 80 °C for 10 min in air. Subsequently, the device was pumped down in vacuum ($<10^{-6}$ Torr), and the Al electrode (thickness ∼100 nm) was deposited. The area of the Al electrode defines the active area of the device as 4.5 mm^2. Thermal annealing was carried out by directly placing the completed devices on a hot plate at 150 °C in a glovebox filled with nitrogen gas. After annealing, the devices were put on a metal plate and cooled to room temperature before the measurements were carried out.

For calibration of the solar simulator, we first carefully minimized the mismatch of the spectrum (the simulating spectrum) obtained from the xenon lamp (300 W Oriel) and the solar spectrum by using an AM1.5G filter. We then calibrated the light intensity by using calibrated standard silicon solar cells with a proactive window made from KG5 filter glass traced to the National Renewable Energy Laboratory. Measurements were done with the solar cells inside the glovebox by using a high-quality optical fiber to guide the light from a solar simulator outside the glovebox. Current density−voltage curves were measured with a Keithley 236 source measurement unit. The characteristics of the solar cells were optimized by testing approximately 100 cells with each [60]methanofullerene derivative. To probe the reproducibility and the trend of the devices with each compound, all the data were reconfirmed by the optimal 10 devices and presented in Tables 2 and 3.

OFET Device Preparation and Measurement. All n-type OFETs were fabricated on heavily doped n-type Si wafers, each covered with a thermally grown silicon oxide (SiO_2) layer with a thickness of 200 nm. The doped Si wafer acts as the gate electrode, and the SiO_2 layer functions as the gate insulator. The active layer was deposited by spin-coating at 2500 rpm. All solutions were prepared at 1 wt% concentration in chlorobenzene. The thickness of the deposited films was about 60 nm. Prior to deposition of source and drain electrodes, the films were dried on hot a plate stabilized at 80 °C for 30 min. All fabrication processes were carried out in the glovebox filled with nitrogen. Source and drain electrodes using Ca were deposited by thermal evaporation by using a shadow mask. The thickness of the source and drain electrodes was 50 nm. Channel length (L) and channel width (W) were 50 μm and 1.5 mm, respectively. All OFET devices were made in the top-contact geometry as shown in Figure 5a. Electrical characterization was performed by using a Keithley semiconductor parametric analyzer (Keithley 4200) under nitrogen atmosphere. The electron mobility (μ) was determined by using the following equation in the saturation regime:

$$I_{ds} = (WC_i/2L)\mu(V_{gs} - V_T)^2$$

where C_i is the capacitance per unit area of the SiO_2 dielectric (C_i = 15 nF/cm^2),and V_T is the threshold voltage.

Synthesis of 4-(2-Ethyl-hexyloxy) Benzoylbutyric Acid (1). Aluminum chloride (41.3 g, 310 mmol) was added in one portion to glutaric anhydride (27.8 g, 232 mmol) and 2-ethylhexyloxy benzene (32 g, 155.3 mmol) in 250 mL of dichloromethane with cooling in an ice−ethanol bath and slowly allowed to warm to room

temperature. The reaction was stirred overnight and then quenched with 2 M HCl; the mixture was then extracted into dichloromethane, washed with brine, and dried. The crude product was chromatographed on silica by using 0−30% ethyl acetate in hexane with 1% acetic acid as eluent and further purified by recrystallization from hexane. Isolated yield = 15.5 g (31%) as white crystals. ^{1}H NMR ($CDCl_3$, 200 MHz): δ ppm 7.94 (d, J = 8.85 Hz, 2H), 6.93 (d, J = 8.85 Hz, 2H), 3.91 (d, J = 5.68 Hz, 1H), 3.03 (t, J = 7.16 Hz, 2H), 2.51 (t, J = 7.08 Hz, 2H), 2.08 (q, J = 6.88 Hz, 2H), 1.73 (m, 1H), 1.55−1.29 (m, 8H), 0.97−0.81 (m, 6H). ^{13}C NMR ($CDCl_3$, 50.28 MHz): δ 197.79, 179.12, 163.18, 130.07, 129.29, 113.99, 70.49, 39.04, 36.72, 32.95, 30.21, 28.81, 23.57, 22.79, 19.03, 13.86, 10.87. HRMS (EI) m/z: 320 ($M^{+\bullet}$). Elemental analysis. Calcd for $C_{19}H_{28}O_4$: C, 71.22; H, 8.81; O, 19.97. Found: C, 71.49; H, 8.71.

Synthesis of Methyl 4-(2-Ethyl-hexyloxy) Benzoylbutyrate (2). A solution of the acid compound **1** (4.0 g, 12.5 mmol) in MeOH (100 mL) with catalytic amount of sulfuric acid (96%, five drops) was refluxed for 5 h. The solvent was evaporated, and the residue was extracted into dichloromethane, washed with brine, and dried. The crude product was chromatographed on silica by using 0−2% ethyl acetate in hexane as eluent. Isolated yield = 4.1 g (98%) as a light yellow liquid. ^{1}H NMR ($CDCl_3$, 200 MHz): δ ppm 7.92 (d, J = 8.95 Hz, 2H), 6.91 (d, J = 8.95 Hz, 2H), 3.89 (d, J = 5.68 Hz, 2H), 3.67 (s, 3H), 2.98 (t, J = 7.17 Hz, 2H), 2.43 (t, J = 7.17 Hz, 2H), 2.05 (p, J = 6.90 Hz, 2H), 1.72 (m, 1H), 1.51−1.27 (m, 8H), 0.97−0.83 (m, 6H). ^{13}C NMR ($CDCl_3$, 50.28 MHz): δ 197.30, 173.12, 162.65, 129.59, 128.92, 113.51, 70.01, 50.89, 38.57, 36.40, 32.54, 29.77, 28.37, 23.11, 22.34, 18.89, 13.42, 10.42. HRMS (EI) m/z: 334 ($M^{+\bullet}$). Elemental analysis. Calcd for $C_{20}H_{30}O_4$: C, 71.82; H, 9.04; O, 19.14. Found: C, 71.73; H, 8.72.

Synthesis of Methyl 4-(2-Ethyl-hexyloxy) Benzoylbutyrate *p*-Tosylhydrazone (3). A mixture of the methyl ester **2** (3.1 g, 9.26 mmol), *p*-toluene-sulfonyl hydrazide (2.07 g, 11.12 mmol), and MeOH (35 mL) with catalytic amount of HCl was stirred and refluxed for 7 h. The mixture was then extracted into dichloromethane, washed with brine, and dried. The crude product was chromatographed on silica by using 0−2% acetone in dichloromethane. Isolated yield = 4.6 g (98%) as a light yellow oil. ^{1}H NMR ($CDCl_3$, 200 MHz): δ ppm 9.02 (s, 1H), 7.92 (d, J = 8.27 Hz, 2H), 7.60 (d, J = 8.89 Hz, 2H), 7.29 (d, J = 9.15 Hz, 2H), 6.85 (d, J = 8.89 Hz, 2H), 3.84 (d, J = 5.67 Hz, 2H), 3.79 (s, 3H), 2.73−2.50 (m, 2H), 2.41 (s, 3H), 2.32 (m, 2H), 1.81−1.62 (m, 3H), 1.52−1.27 (m, 8H), 0.97−0.87 (m, 6H). ^{13}C NMR ($CDCl_3$, 50.28 MHz): δ 174.22, 160.12, 153.26, 143.15, 135.56, 128.97, 127.88, 127.47, 127.15, 113.84, 70.04, 51.89, 38.81, 31.64, 29.99, 28.57, 27.25, 23.33, 22.57, 21.12, 20.58, 13.62, 10.61. HRMS (EI) m/z: 503.25 ($(M + H)^{+\bullet}$). Elemental analysis. Calcd for $C_{27}H_{38}N_2O_5S$: C, 64.51; H, 7.62; N, 5.57; O, 15.91; S, 6.38. Found: C, 64.52; H, 7.52; N, 5.60.

Synthesis of 4-(2-Ethylhexyloxy)-[6,6]-phenyl C_{61}-Butyric Acid Methyl Ester (*p*-EHO-PCBM). A mixture of alkoxy-substituted benzoyl *p*-tosylhydrazone (4.31 g, 8.63 mmol), sodium methoxide (0.485 g, 8.99 mmol), and dry pyridine (50 mL) was placed under argon and stirred at room temperature for 30 min. To the mixture, a solution of C_{60} (5 g, 6.95 mmol) in *o*-DCB (250 mL) was added, and the homogeneous reaction mixture was stirred at 70 °C under argon overnight. The solution was heated to reflux, and the reaction was allowed to continue overnight again. The resulting mixture was concentrated in vacuo to 100 mL and pre-eluted with *o*-DCB (100 mL) and chlorobenzene (200 mL) and then toluene on SiO_2/toluene, 40 × 10 cm. The first fraction, containing unreacted C_{60}, was collected. After an intermediate fraction, the fraction containing 4-(2-ethylhexyloxy)-[6,6]-phenyl C_{61}-butyric acid methyl ester (***p*-EHO-PCBM**) was collected. The solution was concentrated in vacuo, redissolved in a minimal amount of toluene, and transferred to a centrifuge tube. The product was precipitated with MeOH, centrifuged, and decanted. The product was treated with MeOH several times in the same manner and washed with a mixture solution (MeOH:diethylether, 1:1% v/v). Isolated yield = 3.1 g (34%) as a shiny dark solid. ^{1}H NMR ($CDCl_3$, 500 MHz): δ ppm 7.79 (d, J = 8.68 Hz, 2H), 7.03 (d, J = 8.68 Hz, 2H), 3.92 (d, J = 5.53 Hz, 2H), 3.67 (s, 3H), 2.86 (m, 2H), 2.52 (t, J = 7.56 Hz, 2H), 2.17 (m, 2H), 1.76 (m, 1H), 1.61−1.30 (m, 8H), 0.97−0.87 (m, 6H). ^{13}C NMR ($CDCl_3$, 125.70 MHz): δ 173.43, 158.93, 148.83, 147.89, 145.77, 145.06, 145.00, 144.90, 144.66, 144.59, 144.53, 144.35, 144.27, 143.87, 143.64, 142.91, 142.86, 142.78, 142.13, 141.99, 140.82, 140.59, 137.87, 137.58, 132.97, 128.05, 114.21, 80.13, 70.42, 51.58, 51.28, 39.38, 33.81, 33.65, 30.48, 29.06, 23.79, 22.99, 14.05, 11.12. FABMS (NBA) m/z: 1040 ($(M + H)^{+\bullet}$). Elemental analysis. Calcd for $C_{80}H_{30}O_3$: C, 92.47; H, 2.91; O, 4.62. Found: C, 92.53; H, 2.74.

Synthesis of 4-(2-Ethylhexyloxy)-[6,6]-phenyl C_{61}-Butyric Acid Methyl Ester (*p*-EHO-PCBA). A sample of ***p*-EHO-PCBM** (1.5 g, 1.44 mmol) was dissolved in chlorobenzene, and to this solution were added acetic acid (100 mL) and concentrated aqueous HCl (40 mL). The mixture was heated to reflux overnight. The solvent was removed in vacuo, and the residue was suspended in methanol. The precipitate was collected by filtration, washed three times with methanol and twice with a mixture solution (MeOH: diethylether, 1:1% v/v), and dried. Isolated yield = 1.42 g (96%) as a brown solid. ^{1}H NMR ($CDCl_3$, 500 MHz): δ ppm 7.79 (d, J = 8.50 Hz, 2H), 7.03 (d, J = 8.48 Hz, 2H), 3.91 (d, J = 5.70 Hz, 2H), 2.95−2.79 (m, 2H), 2.55 (t, J = 7.31, 2H), 2.19 (m, 2H), 1.77 (m, 1H), 1.60−1.28 (m, 8H), 0.97−0.85 (m, 6H). ^{13}C NMR ($CDCl_3$, 125.70 MHz): δ 178.61, 159.05, 148.86, 147.90, 145.87, 145.14, 145.11, 144.78, 144.72, 144.69, 144.62, 144.45, 144.37, 143.98, 143.72, 143.06, 142.99, 142.95, 142.89, 142.23, 142.19, 142.10, 140.93, 140.68, 138.00, 137.69, 133.03, 128.10, 114.34, 80.18 (bridge), 70.56, 51.29, 39.48, 33.67, 33.62, 30.57, 29.15, 23.89, 23.08, 22.21, 14.15, 11.12. FABMS (NBA) m/z: 1025 ($(M + H)^{+\bullet}$). Elemental analysis. Calcd for $C_{79}H_{28}O_3$: C, 92.56; H, 2.75; O, 4.68. Found: C, 92.88; H, 3.18.

Acknowledgment. Synthesis and characterization was supported by MC-CAM. Device fabrication and measurement was supported by the Air Force Office of Scientific Research (Charles Lee, Program Officer) and by the U.S. Department of Energy (A. Kini, Program Officer).

Supporting Information Available: ^{1}H and ^{13}C NMR spectra for all new compounds and cyclic voltammograms of C_{60}, PCBM, ***p*-EHO-PCBM**, and ***p*-EHO-PCBA**. This material is available free of charge via the Internet at http://pubs.acs.org.

JA710621J